



## What is the real gas gain of a standard GEM?

R. Bellazzini\*, A. Brez, G. Gariano, L. Latronico, N. Lumb, G. Spandre,  
M.M. Massai, R. Raffo, M.A. Spezziga

*INFN-Pisa and University of Pisa, Via Livronese 582/A, I-56010 S. piero a Grado, Pisa, Italy*

---

### Abstract

We have observed very high gains (up to 7000) from GEMs with 'standard' parameters (kapton thickness 50  $\mu\text{m}$ , pitch 120  $\mu\text{m}$ , copper hole diameter 65  $\mu\text{m}$ , kapton hole diameter 30  $\mu\text{m}$ ). This was achieved using GEMs coupled to a simple array of copper read-out strips. From the measurements of the current on all the electrodes, we conclude that the high observed gains are fully attributable to electron multiplication in the holes of the mesh, and not to electronics related effects as had been previously suggested. Furthermore, we report that this large gain may only be fully exploited when the field in the second GEM gap is high. The effect on the gain of coupling a GEM to another charge amplifying device was investigated using a GEM-PMGC combination. © 1998 Elsevier Science B.V. All rights reserved.

*Keywords:* Kapton layer; Gas electron multiplier

---

### 1. Introduction

The field of gas proportional wire counters has been revolutionised by the introduction of micro-electronics technology or advanced printed circuit technology to define micro-pattern structures around which sizable gas gain can be obtained. Examples of new detectors which take advantage of these techniques are Micro-Strip Gas Chambers (MSGCs), Micro-Gap Chambers (MGCs), Small Gap Chambers (SGCs), MICROMEGAS, Microdots, and the Compteur A Trou (CAT) [1]. One of the most promising additions to this list is the Gas Electron Multiplier (GEM) [2].

The GEM consists of a thin kapton foil, copper coated on both sides and perforated by a regular pattern of closely spaced holes. The chemical etching process [3] used to produce the holes creates openings with a double-conical profile [4], wider in the metal layers than in the insulator. The GEM is placed between parallel drift and collection electrode planes which also serve to delimit the gas envelope. Application of a suitably high potential between the metal layers of the GEM produces an electric field in the holes sufficient for electron multiplication. The collection electrodes may be simple copper strips produced using printed circuit board technology, or a further amplifying structure such as a multi-wire proportional counter or an MSGC. We refer to the type of GEM described above as a 'standard' GEM, in contrast to devices in which the gain is enhanced by placing two meshes in

---

\*Corresponding author. E-mail: bellazzini@pisa.infn.it.

cascade at some distance (Double-GEM) or in electrical contact (Super-GEM) [5].

The aim of this paper is to show how, by simultaneously measuring particle rates and the currents on all four GEM electrodes, it is possible to unambiguously determine the real gas gain of the GEM itself. We also discuss methods and conditions to fully exploit this gain.

## 2. Experimental set-up

The experimental arrangement is shown in Fig. 1. We studied GEMs with hole diameters of  $30\ \mu\text{m}$  in the middle of the kapton layer and  $65\ \mu\text{m}$  in the metal layers, the spacing between hole centres being  $120\ \mu\text{m}$ . The thickness of the kapton layer was  $50\ \mu\text{m}$  and the overall dimensions of the GEM were  $2.5\ \text{cm} \times 2.5\ \text{cm}$ . Initially, the drift and collection planes were separated from the GEM by spacers of thickness 3 mm, but in later tests the collection gap was reduced to 1 mm. The gas mixture was Ne/DME, 50/50. A printed circuit board with copper strips (pitch: 1.6 mm) was used for the collection plane, and the drift electrode was an aluminised mylar sheet. The current flowing in the connections to all four electrodes were monitored using picoammeters.

We define:

$I_D$  = current from drift window.

$I_{G-}$  = current from upper (most negative) GEM electrode.

$I_{G+}$  = current from lower (most positive) GEM electrode.

$I_C$  = current from collection electrodes.

## 3. Results and interpretation

### 3.1. Signal shape

The potential difference across the GEM electrodes was set at 500 V. The drift field (field between the drift electrode and the most negative GEM electrode) was fixed at  $3.3\ \text{kV/cm}$  and the collection field (between the most positive GEM electrode and the collection plane) was set to  $10\ \text{kV/cm}$ . The chamber was irradiated with  $5.4\ \text{keV}$  X-rays at an absorbed photon rate of approximately  $10^5\ \text{Hz}$ . The X-ray beam was collimated to a diameter of about 1 mm, ensuring that most of the avalanche charge was collected on a single read-out strip.

Examples of pulses seen on the collection strips are displayed in Fig. 2, for collection gaps of (a) 3 mm and (b) 1 mm. An example of the signal as seen on an analogue oscilloscope is also shown (c).

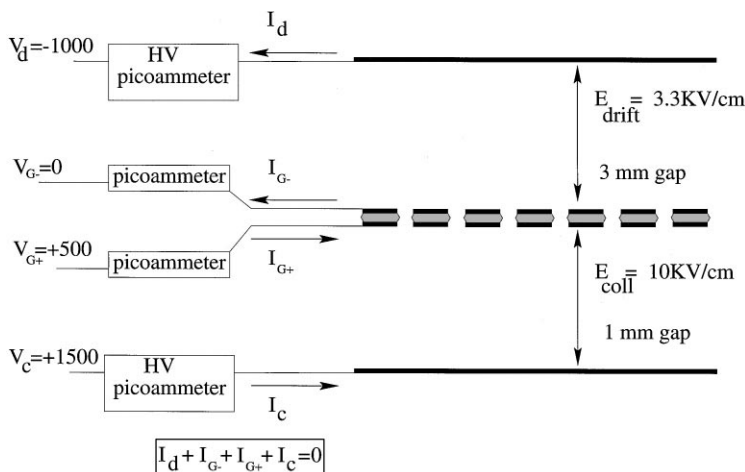


Fig. 1. Arrangement for studying currents in a GEM-based detector.

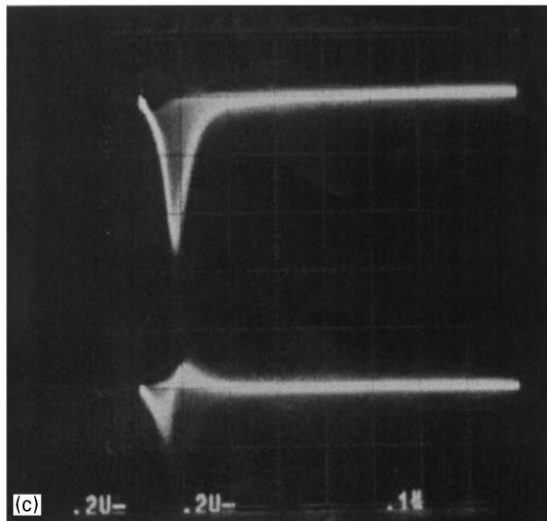
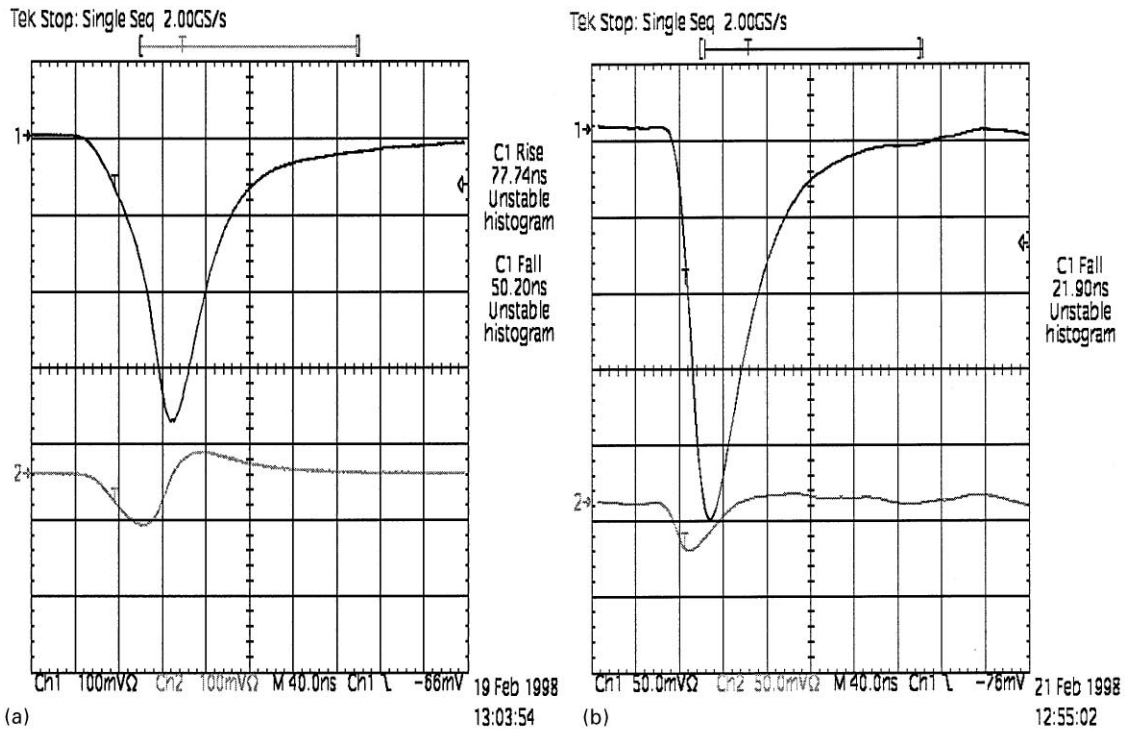


Fig. 2. Pulses observed using a digitising oscilloscope, for collection gaps of (a) 3 mm and (b) 1 mm; analogue signals (c).

The shaping time of the amplifiers was 50 ns. The signal from an adjacent strip is also shown in each case. Note that these signals are bi-polar, reflecting the fact that charge induced on the strips adjacent

to the collection strip has to be ‘returned’ upon collection of the avalanche. Fig. 2 clearly shows how the rise time of the signal may be reduced by narrowing the collection gap.

### 3.2. Electrical transparency

For applications in which the number of primary electrons is relatively low (e.g. in the detection of minimum ionising particles), the *transparency* of the GEM mesh is an important consideration. Here we define transparency to be the fraction of primary electrons which pass through a GEM hole, producing an avalanche. The value of this fraction depends on both the *optical* and *electrical* transparency of the mesh. The optical transparency is determined by the ratio of the ‘open’ area of the mesh to the total area. The electrical transparency is defined by the proportion of field lines passing through the GEM holes (in contrast to those which terminate on the upper GEM electrode) and is controlled by the strength of the field in the drift region relative to that in the holes.

The electrical transparency of the GEM was studied by measuring the signal current while varying the drift field from 0 to 10 kV/cm, with the collection field fixed at 4.5 kV/cm and the GEM potential at 500 V. The results of this study are shown in Fig. 3, in which the relative transparency is defined as  $I_C/I_C^{\max}$ . We interpret the plot as follows. For low drift fields, the probability of ion-electron recombination is rather high and this fact is reflected in the small signal current. For very high drift fields, the concentration of field lines in the drift gap is high and the probability of some of these lines ending on the metal of the upper GEM

electrode is enhanced. Hence the overall effect is to produce a maximum in the transparency curve. For the case of the GEM studied, this maximum was attained using a drift field of around 4 kV/cm.

The relative transparency at 10 kV/cm is 70% of the maximum. The absolute transparency must certainly be a lower percentage of the maximum, since in these measurements we were unable to de-couple the effect of the increase in GEM gain produced by increasing the drift field.

The energy resolution of the GEM was also measured as a function of the drift field, see Fig. 3. The best energy resolution was achieved at the maximum transparency, and was 26% FWHM.

### 3.3. Effect of varying the collection field

The effect produced on the distribution of currents to the electrodes by varying the collection field was investigated. The collection field was varied with the drift field set at 3.3 kV/cm and a constant potential difference of 500 V across the GEM. The results of this test are summarised in Fig. 4 and we interpret them as follows.

Ions produced in an avalanche may be collected either by the drift electrode or by the upper GEM electrode. Electrons from the avalanche drift towards the collection strips and produce the signal we require to extract position information. However, field lines from the multiplication region may also end on the lower GEM electrode, allowing

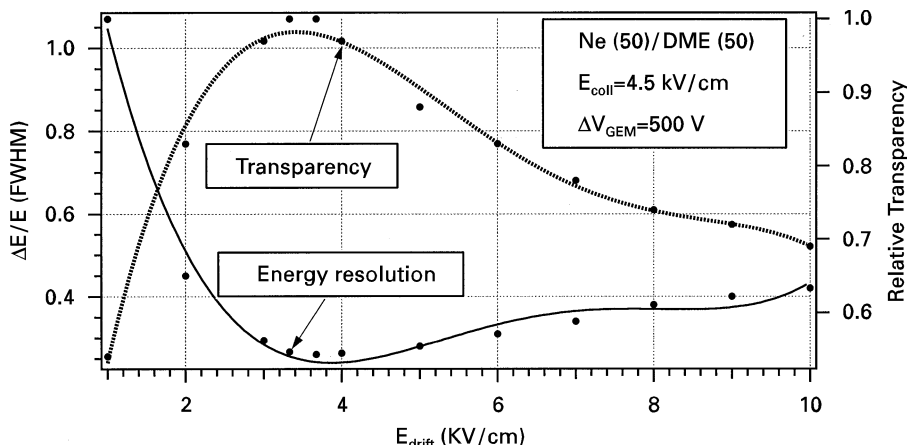


Fig. 3. Relative signal current ( $I_C/I_C^{\max}$ ) and energy resolution for varying drift field; all other field parameters constant.

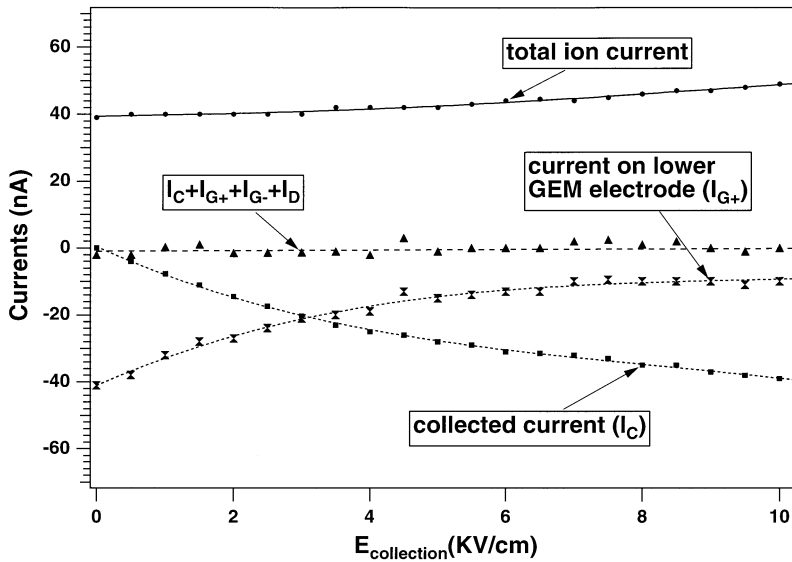


Fig. 4. Dependence of electrode currents on collection field strength.

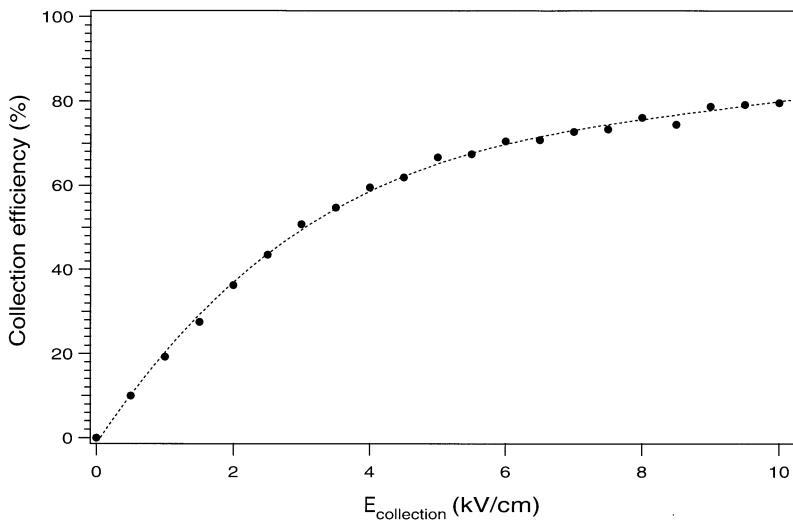


Fig. 5. Collection efficiency as a function of collection field strength.

electrons to be collected there and inducing a corresponding current. Indeed, from Fig. 4, we see that for low collection fields, most of the avalanche electrons are deposited on this electrode. Only by applying a high collection field can we ensure that most of the signal current appears on the read-out

strips. A plot of collection efficiency ( $I_C/[I_C + I_{G+}]$ ) against collection field (Fig. 5) shows that an efficiency of 80% can be reached with  $E_{\text{coll}} = 10$  kV/cm.

We expect the sum of all four electrode currents to be zero always, and we see from Fig. 4 that this is indeed the case. Note that the total ion current

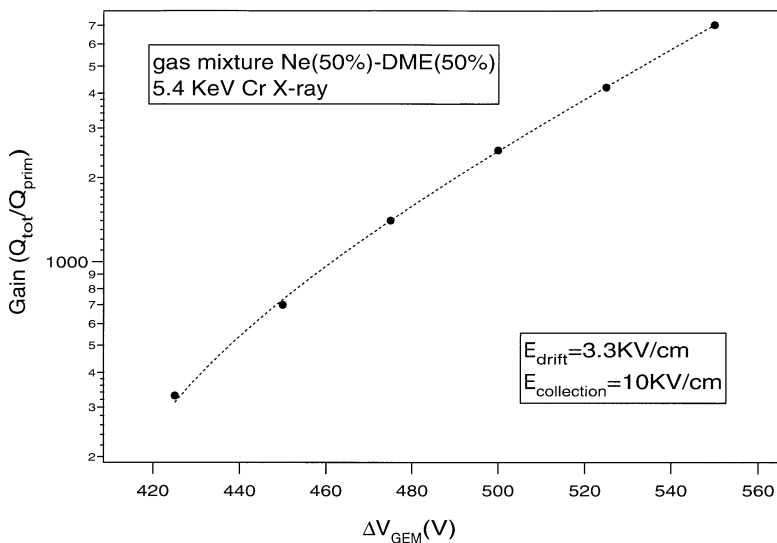


Fig. 6. Dependence of gain upon GEM voltage.

( $I_D + I_{G-}$ ) increases gradually with increasing collection field. This is due to slight enhancement of the multiplication field by the collection field.

### 3.4. GEM gain

The gain of the GEM was studied by measuring the signal current for various potential differences across the GEM electrodes, keeping the external fields at constant, optimised values ( $E_{\text{drift}} = 3.3 \text{ kV/cm}$ ,  $E_{\text{coll}} = 10 \text{ kV/cm}$ ). Knowing the rate of the irradiating photons ( $10^5 \text{ Hz}$ ,  $5.4 \text{ keV Cr X-rays}$ ), and assuming a primary ionisation charge of 200 electrons, the currents could be converted to gain values,<sup>1</sup> see Fig. 6. We observe a GEM gain of well above 2000 for  $\Delta V_{\text{GEM}} = 500 \text{ V}$ , and a maximum gain of 7000 for  $\Delta V_{\text{GEM}} = 560 \text{ V}$  (the measured collection current became unstable at higher gains). These values were confirmed by the measurement of pulse heights from our calibrated electronics. Another group reported lower implied GEM gains (about 100 for  $\Delta V_{\text{GEM}} = 500 \text{ V}$ ), using similar

GEMs but using an MSGC to provide further amplification [5]. However, high gains in agreement with our results are indicated in their work ([5], Fig. 10) for the case when the MSGC amplification was removed by lowering the MSGC cathode voltage to 0 V. At that time the high gain of the GEM alone was defined as ‘apparent’ and explained in terms of electronics effects (absence of ballistic deficit since signal is induced by electrons, no cross-talk). We suggest that such an explanation is inadequate and that in fact the gain of this type of GEM is real and is at least an order of magnitude higher than had been previously assumed.

### 3.5. GEM coupled to a PMGC

The apparent reduction of the GEM gain by the inclusion of a further amplification stage may be better explained by a combination of effects which we have observed experimentally. First, when working with low collection fields, the collection efficiency is significantly reduced as the MSGC cathode voltage is increased to high negative values. To investigate this effect, we have coupled a Planar Micro Gap Detector (PMGC) – an MSGC with very narrow anode–cathode gap, see

<sup>1</sup>  $I_{\text{tot}} = I_C + I_{G+} = \text{Rate} * \text{Gain} * Q_{\text{primary}}$ .

Ref. [6] – and a GEM and measured the overall gain as a function of the PMGC cathode voltage. The drift field was set at the optimum value of 4 kV/cm (see Section 3.2) and the GEM voltage was 540 V. The initial collection field (i.e. for 0 V on the PMGC cathodes) was chosen to be rather low (540 V over 3 mm gap = 1800 V/cm). It can be seen from Fig. 5 that the collection efficiency corresponding to this field is about 25%. In Fig. 7 we plot the gain of the GEM–PMGC combination, calculated from the measured PMGC anode current, for increasing PMGC cathode voltage. When the cathode voltage is below about 100 V, the PMGC does not yet produce amplification and its electrodes serve only to collect the electrons produced in the GEM avalanches. As the cathode voltage approaches zero, most of the charge is collected on the cathodes (which are much wider than the anode strips) and the anode current falls (dashed line in Fig. 7). We can correct this region of the graph by also measuring the cathode current and calculating the gain from the sum of the two currents (solid line). The visible gain of the GEM alone is, then, around 800 (here we use the term ‘visible gain’ to mean the gain calculated by considering avalanche electrons which are transferred to the collection gap, neglecting those which follow field lines ending on the lower GEM electrode). The

gain of the PMGC alone, with cathode volts at 380 V is approximately 1000. From Fig. 7 the implied gain of the GEM (total gain/PMGC gain) is only about 4 for  $V_c = 380$  V. Alternatively, we can say that the overall gain of the coupled devices is a factor 200 lower, than we expect from simply multiplying their independently measured gains. This is partly explained by the fact that the collection field strength has been reduced to about 600 V/cm by the increase in the cathode potential, lowering the collection efficiency from the original 25% to only about 5%.

The second effect which we have investigated is gain reduction by space charging produced by the enormous number of electrons in the MSGC or PMGC avalanche. To eliminate the first effect discussed above, we worked with a high collection field (between 8 and 10 kV/cm). The visible gain of the coupled GEM and PMGC was calculated from anode current measurements and compared with the independently measured visible gain of the GEM and the gain of the PMGC. These data are displayed in Fig. 8 as a function of cathode voltage (or voltage across the GEM for the ‘GEM alone’ curve). Two sets of data were taken for the coupled system, corresponding to two different GEM voltages (420 and 500 V). A change of slope indicating a saturation effect

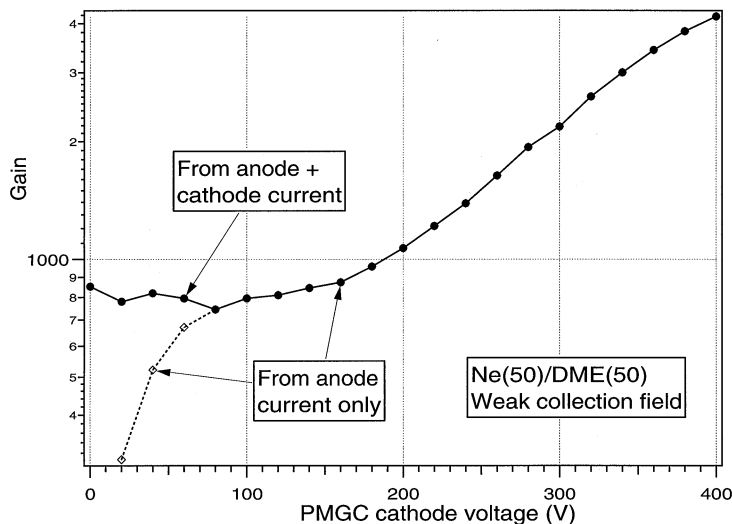


Fig. 7. Gain for a coupled GEM–PMGC system with low collection field.

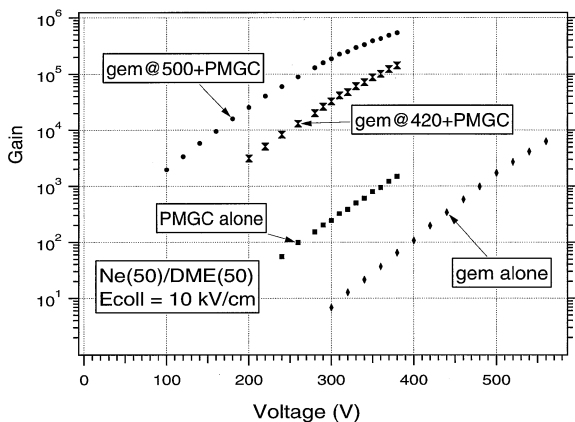


Fig. 8. Gains of two GEM–PMGC systems with high collection field, and of the de-coupled amplifying elements.

is evident in these data, starting from a PMGC cathode voltage of about 300 V.

In Fig. 9, we plot the ratio (Gain of coupled devices)/(Gain of GEM alone \* Gain of PMGC alone). The coupled system provides a smaller fraction of the expected gain as the PMGC cathode voltage is increased, or as the GEM voltage is raised. We suggest that this is a space-charge effect occurring in the vicinity of the PMGC anodes and/or the GEM holes.

In summary, we have studied a combined GEM/PMGC system in which the overall gain of the system was lower than expected. This phenomenon had been reported elsewhere [5]. We chose conditions designed to exacerbate the effect and observed an apparent factor 200 ‘loss’ of gain. A factor 5 is explained by reduction of the collection efficiency as the PMGC cathode voltage was increased. Space-charge effects contribute a further factor 2 or 3. The origin of the remaining factor of 15–20 present in this worst-case configuration is not clear. One possible explanation is that when working with very low collection fields there is inefficient transport of electrons (recombination, capture by gas molecules) across the 3 mm collection gap used for this part of our work. (The collection efficiency data presented in Fig. 5 were taken using a 1 mm gap.) Despite our incomplete understanding, the main message is clear: in order to exploit fully the gain achievable by combining

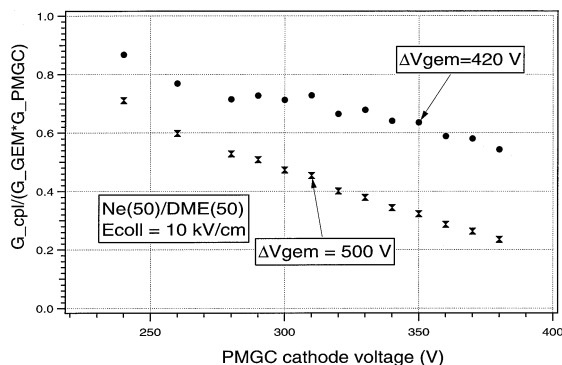


Fig. 9. Observed fraction of expected gain for two GEM–PMGC systems with high collection field.  $G_{cpl}$  is the measured gain of the coupled devices;  $G_{GEM}$  and  $G_{PMGC}$  are the gains of the GEM and PMGC alone.

a GEM with another charge amplifying device, the collection field used should be as high as possible.

#### 4. Conclusions

The gas gain of a standard GEM operated without a further amplification stage is higher than had previously been imagined. For example, for a potential difference of 500 V across the GEM electrodes, gains above 2000 are routinely achieved.

The electron avalanche charge is always collected by at least two electrodes: *the GEM itself* and an additional collecting electrode at a more positive voltage. The fraction of ‘visible’ gain detected on the additional electrode can range from 0 to 80%, depending on the collecting field (0–10 kV/cm). Large and fast signals can be detected on the strips of the collecting electrode; this is related to the gain collection efficiency and not to electronics effects.

When a GEM is combined with another charge amplifying structure such as an MSGC or a PMGC, the total observed gain may be significantly lower than the combined gains of the de-coupled devices. This effect is most evident when the GEM is operated with a weak collection field, and/or when operating at very large gains (space charging).



We envisage many interesting applications for the GEM when working in collection mode (using optimised potentials to give high collection efficiency).

### Acknowledgements

We would like to acknowledge the assistance of A. Gandi, R. De Oliveira and L. Mastrostefano of the CERN advanced printed circuit workshop. This work would not have been possible without their skill and experience in the production of GEM electrode structures.

### References

- [1] F. Sauli, Nucl. Instr. and Meth. A 419 (1998) 189.
- [2] F. Sauli, Nucl. Instr. and Meth. A 386 (1997) 531.
- [3] A. Gandi et al., Manufacturing procedures for the gas electron multiplier, in preparation at CERN, 1997.
- [4] R. Bouclier et al., New Observations with the Gas Electron Multiplier, CERN-PPE/97-32, 1997.
- [5] J. Benlloch et al., Development of the gas electron multiplier, CERN-PPE/97-146, 1997.
- [6] R. Bellazzini et al., Nucl. Instr. and Meth. A 409 (1998) 14.